Circulation
JOURNAL OF THE AMERICAN HEART ASSOCIATION



# Bionic Technology Revitalizes Native Baroreflex Function in Rats With Baroreflex Failure

Takayuki Sato, Toru Kawada, Masaru Sugimachi and Kenji Sunagawa

*Circulation* 2002;106;730-734; originally published online Jul 15, 2002;
DOI: 10.1161/01.CIR.0000024101.77521.4D
Circulation is published by the American Heart Association. 7272 Greenville Avenue, Dallas, TX 72514
 Print ISSN: 0009-7322. Online ISSN: 1524-4539

# Bionic Technology Revitalizes Native Baroreflex Function in Rats With Baroreflex Failure

Takayuki Sato, MD; Toru Kawada, MD; Masaru Sugimachi, MD; Kenji Sunagawa, MD

***Background*—**We developed a bionic technology for the treatment of baroreflex failure and tested its efficacy in restoration of arterial pressure against head-up tilt (HUT) in rats with baroreflex failure.

***Methods and Results*—**The bionic baroreflex system (BBS) was a negative feedback system controlled by a computer, the artificial vasomotor center. It sensed systemic arterial pressure (SAP) through a micromanometer placed in the aortic arch and automatically computed the frequency of a pulse train to stimulate sympathetic efferent nerves. We selected the celiac ganglion as the sympathetic vasomotor interface. To make this system bionic, the operational rule of the artificial vasomotor center ($H_{BRP\rightarrow STM}$; BRP indicates baroreceptor pressure; STM, electrical stimulation) was actively matched to that of the native center. First, we identified the open-loop transfer functions of the native baroreflex control of SAP ($H_{Native}$) and the response of SAP to electrical stimulation of the celiac ganglion ($H_{STM\rightarrow SAP}$). We computed $H_{BRP\rightarrow STM}$ from $H_{Native}/H_{STM\rightarrow SAP}$ and transplanted the operational rule into the computer. In 10 rats with baroreflex failure, we evaluated the performance of the BBS during rapid hypotension induced by HUT. Abrupt HUT dropped SAP by $34\pm6$ mm Hg in 2 seconds and by $52\pm5$ mm Hg in 10 seconds. During real-time execution of the BBS, on the other hand, the fall in SAP was $21\pm5$ mm Hg at 2 seconds and $15\pm6$ mm Hg at 10 seconds after HUT. These arterial responses controlled by the BBS were indistinguishable from those by the native baroreflex.

***Conclusions*—**We concluded that the BBS revitalized the native baroreflex function in rats with baroreflex failure. **(*Circulation*. 2002;106:730-734.)**

**Key Words:** baroreceptors ■ blood pressure ■ dynamics ■ electrical stimulation ■ nervous system, sympathetic

The most unique function of arterial baroreflex is to quickly and sufficiently attenuate the effect of an external disturbance on arterial pressure.[1–3] Without such quick compensation, the simple act of standing would cause a fall in arterial pressure responsible for perfusing the brain, resulting potentially in loss of consciousness. Therefore, the functional restoration of dynamic as well as static properties of the arterial baroreflex is essential to patients with baroreflex failure.[4–6]

Neurological disorders such as Shy-Drager syndrome,[7–10] baroreceptor deafferentation,[11,12] and traumatic spinal cord injuries[13,14] result in central baroreflex failure and a severely impaired quality of life as a consequence. In Shy-Drager syndrome, idiopathic neurodegeneration affects the vasomotor center in the brain stem; however, peripheral sympathetic neurons are assumed to be relatively spared and able to release norepinephrine in response to excitatory outflow. In spinal cord injuries, sympathetic traffic to preganglionic neurons can be interrupted permanently. In either case, peripheral sympathetic neurons have the ability to release norepinephrine in response to direct electrical stimuli.[10] Unfortunately, although various interventions such as salt loading,[15,16] cardiac pacing,[17,18] and adrenergic agonists[19,20] have been attempted to treat orthostatic hypotension, most patients nevertheless remain bedridden for a long time. The reason for this unfortunate outcome is that such interventions can neither restore nor reproduce the functioning of the native vasomotor center.

In our previous study,[21] we developed a framework for identifying an operational rule of the vasomotor center and a prototype of a bionic baroreflex system in rats. The bionic system is an artificial device for functional replacement of a physiological system able to mimic its static and dynamic characteristics. The objective of the present study is to evaluate the efficacy of our bionic system in an animal model of central baroreflex failure.

## Methods

### Theoretical Considerations

Provided in Figure 1A is a simplified diagram representing characteristics of the native baroreflex system. The vasomotor center responsively modifies its command over sympathetic vasomotor nerve activity according to changes in baroreceptor pressure (BRP). Efferent sympathetic nerve activity in turn governs the functional

Received March 13, 2002; revision received May 8, 2002; accepted May 9, 2002.

From the Department of Cardiovascular Dynamics (T.S., T.K., M.S., K.S.), National Cardiovascular Center Research Institute, Suita, Japan; and the Department of Cardiovascular Control (T.S.), Kochi Medical School, Nankoku, Japan.

Correspondence to Dr Takayuki Sato, Department of Cardiovascular Control, Kochi Medical School, Nankoku, Kochi 783-8505, Japan. E-mail tacsato-kochimed@umin.ac.jp



*Circulation* is available at http://www.circulationaha.org

DOI: 10.1161/01.CIR.0000024101.77521.4D

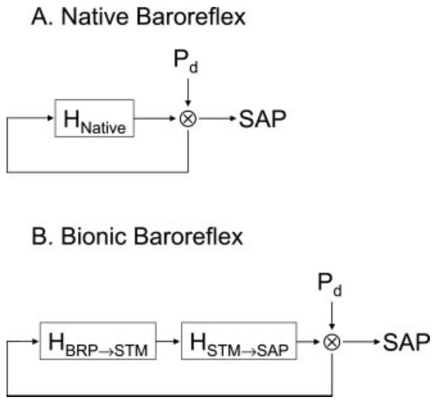


**Figure 1.** Block diagrams of native (A) and bionic (B) baroreflex systems. In the native baroreflex system, a change in SAP induced by external disturbance in pressure ($P_d$) is sensed by arterial baroreceptors. Change in BRP initiates reflex change in vasomotor sympathetic outflow and is thereby buffered. In the bionic baroreflex system, a catheter-tipped micromanometer functions as the baroreceptor, a computer as the vasomotor center, and an electrical stimulator as the preganglionic sympathetic neuron. $H_{Native}$ denotes the open-loop transfer function of the native baroreflex system. $H_{BRP \rightarrow STM}$ and $H_{STM \rightarrow SAP}$ are the open-loop transfer functions from BRP to the frequency of STM and from STM to SAP, respectively. Overall open-loop transfer function of the bionic baroreflex system is given by $H_{BRP \rightarrow STM} \times H_{STM \rightarrow SAP}$.

properties of various effectors, such as resistive and capacitive vessels, which themselves exert direct influence over systemic arterial pressure (SAP). Although the effect of a postural change is added to SAP as a pressure disturbance, $P_d$, the change in SAP, is attenuated to $P_d/(1+|H_{Native}|)$. Here $H_{Native}$ is the transfer function[22,23] of the native baroreflex system.

On the other hand, in the bionic baroreflex system (BBS), BRP is sensed by a catheter-tipped micromanometer placed in the aortic arch and fed into a computer that functions as an artificial vasomotor center. On the basis of measured changes in SAP, the artificial vasomotor center executes real-time operations that determine the frequency of electrical stimulation (STM) necessary for compensatory adjustment of SAP to the desired level and then commands an electrical stimulator to provide a stimulus of the same frequency to the vasomotor sympathetic nerves. To enable the BBS to effectively mimic the functioning of the native baroreflex system, it is necessary to identify quantitatively the operating rule that underlies native baroreflex function and to implant it into the BBS. According to the following procedures (Figure 1B), we can identify the transfer function of $H_{Native}$.

We first analyze under open-loop conditions the BRP-SAP dynamic properties characterizing $H_{Native}$ by using a white-noise identification method. Next, we identify the open-loop transfer function ($H_{STM \rightarrow SAP}$) from STM to SAP. The determination of $H_{STM \rightarrow SAP}$ enables us by a simple process of division, $H_{Native}/H_{STM \rightarrow SAP}$, to calculate the open-loop transfer function required for the artificial vasomotor center of the BBS, that is, $H_{BRP \rightarrow STM}$. The transfer function $H_{BRP \rightarrow STM}$ represents the operating rule characterizing quantitatively the dynamics of how the artificial vasomotor center should operate in its stimulation of the vasomotor sympathetic nerves to mimic the native baroreflex.

## Animals and Surgical Procedures

The care of animals was in strict accordance with the guiding principles of the Physiological Society of Japan. A total of 10 male Sprague-Dawley rats (SLC, Hamamatsu, Japan) weighing 280 to 350 g were used. The rat was ventilated artificially by means of a volume-controlled rodent respirator (model 683, Harvard Apparatus) at 80 strokes per minute. Anesthesia was maintained through the use of 1.2% halothane during surgical procedures and 0.6% halothane during data recording. Polyethylene tubings (PE-10, Becton Dickinson) were inserted into the right femoral vein and the left common carotid artery. Pancuronium bromide (0.8 mg/kg per hour IV) was administered to eliminate spontaneous muscle activity. Arterial blood gases were monitored with a blood gas analyzer. For the prevention of dehydration during experiments, physiological saline was continuously infused at a rate of 5 mL/kg per hour with a syringe pump. For measurement of SAP, a 2-F catheter-tipped micromanometer (SPC-320, Millar Instruments) was placed in the aortic arch through the right femoral artery.

To open the feedback loop of the arterial baroreflex system, we cut the vagi and the aortic depressor nerves and isolated the carotid sinus baroreceptor regions by the embolization method.[24] Two short polyethylene tubings (PE-50) were placed into both carotid sinuses and connected to a fluid-filled transducer (DX-200, Viggo-Spectramed) and to a custom-made servo-controlled pump system. We used the servo-controlled pump to impose various pressures on carotid sinus baroreceptor regions.[6]

We selected the celiac ganglion[25] as the vasomotor sympathetic nerve interface for the BBS because the abdominal splanchnic vascular bed innervated by the ganglion has been shown to be a major effector mechanism for the arterial baroreflex.[26,27] The left greater splanchnic nerve was identified, separated free, and cut at the level of the diaphragm through a left flank incision. A pair of Teflon-coated platinum wires (7720, A-M Systems) was looped around and fixed on the distal end of the nerve. The implantation site of the wires was embedded in silicone rubber. The free ends of the wires were connected to an isolated constant-voltage stimulator (SS-202J and SEN-7203, Nihon Kohden) controlled with a dedicated laboratory computer (PC-9801RA21, NEC). Finally, the flank incision was closed in layers.

## Data Recording for Estimation of $H_{Native}$

To estimate the open-loop transfer function $H_{Native}$, we randomly altered carotid sinus BRP between 100 to 120 mm Hg with a white bandwidth up to 2 Hz by using the servo-controlled pump system. While the random perturbation was given for an hour, the electrical signals of BRP and SAP were first low-pass–filtered with antialiasing filters having a cutoff frequency of 50 Hz (−3 dB) and an attenuation slope of −80 dB per decade and then digitized at a rate of 100 Hz by means of an analog-to-digital converter.

## Data Recording for Estimation of $H_{STM \rightarrow SAP}$

To estimate the open-loop transfer function $H_{STM \rightarrow SAP}$, we randomly changed STM between 0 to 10 Hz with white noise with a bandwidth up to 2 Hz while BRP was kept at a constant pressure of 120 mm Hg. The pulse width of the stimulus was fixed at 2 ms. The stimulation voltage was adjusted for each animal to produce a pressor response of 40 mm Hg at 10 Hz. This resulted in an average amplitude of $4.2 \pm 0.3$ (mean±SD) V. While the random perturbation was given for 1 hour, STM and SAP were digitized at a rate of 100 Hz.

## Estimation of Transfer Function

The transfer function $H_{x \rightarrow y}$ from input $x$ to output $y$ was estimated with a fast Fourier transform algorithm.[22,23,28] The digitized data of $x$ and $y$ were resampled at 2 Hz after a moving average to avoid aliasing. The time series of each data were divided into 50 segments of 256 points each, with 128 points of overlap between segments. To suppress spectral leakage, we applied a Hann window to each segment and then computed the raw autospectra of $x$ and $y$ and the raw cross spectrum between the two. To reduce an error in estimating the spectrum, we calculated the ensemble average of 50 raw spectra. Finally, we computed the transfer function over the frequency range of 0.008 to 1 Hz as follows:

$$H_{x \rightarrow y} = \frac{S_{xy}}{S_{xx}},$$

where $S_{xx}$ is the ensembled autospectrum of $x$ and $S_{xy}$ is the ensembled cross spectrum of $x$ and $y$. $H_{x \rightarrow y}$ is, in general, a complex quantity and is therefore expressible in polar form as

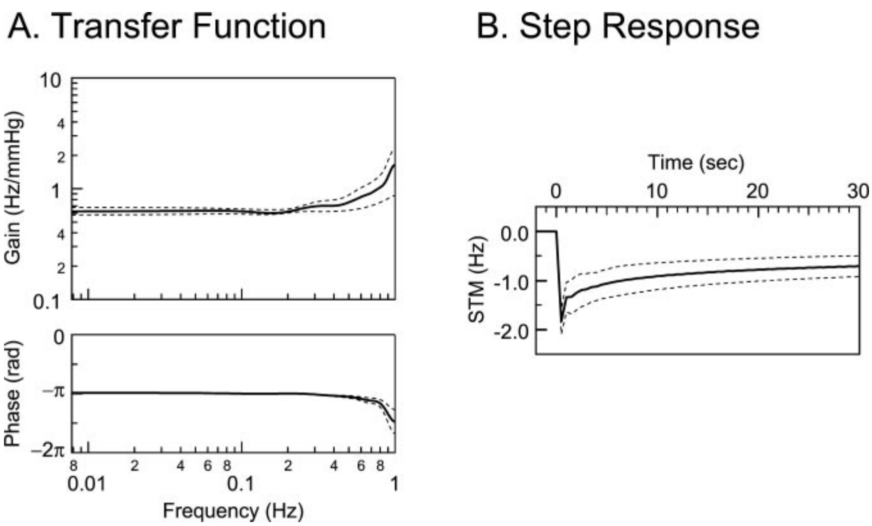


**Figure 2.** Open-loop transfer function (A) required for artificial vasomotor center of the bionic baroreflex system and step response (B) computed from transfer function. Data are expressed as mean±SD for 10 rats. See text for explanation.

$$H_{x\to y}=|H_{x\to y}|\exp\{j\phi_{x\to y}\},$$

where $j^2=-1$, and $|H_{x\to y}|$ and $\phi_{x\to y}$ are the gain and phase of the transfer function, respectively. The squared coherence function, a measure of linear dependence between $x$ and $y$, was estimated with the following equation:

$$\mathrm{coh}=\frac{|S_{xy}|^2}{S_{xx}\times S_{jj}}$$

where $S_{yy}$ is the ensembled autospectrum of $y$.

### Implantation of $H_{BRP\to STM}$ Into BBS

The open-loop transfer function required for the artificial vasomotor center, $H_{BRP\to STM}$, was determined by a simple process of division, $H_{Native}/H_{STM\to SAP}$. To make the BBS computer operate in real time as the artificial vasomotor center, we programmed the computer to automatically calculate instantaneous STM in response to instantaneous BRP change according to a convolution algorithm[22]:

$$\mathrm{STM}(t)=\int_0^\infty h(\tau)\cdot \mathrm{BRP}(t-\tau)d\tau$$

where $h(t)$ is an impulse response function computed by an inverse Fourier transform of $H_{BRP\to STM}$.

### Head-Up Tilt Tests

We restrained the rat on a custom-made tilt table. To evaluate the efficacy of the BBS against orthostatic hypotension caused by central baroreflex failure, we measured SAP responses of each rat to head-up tilting (HUT) under 3 experimental conditions. For each animal, 3 trials of measurement under each condition were made in random order.

First, to mimic orthostatic hypotension in central baroreflex failure, we kept BRP constant at the same level as SAP in a supine position before and after HUT. We referred to this condition as the model of central baroreflex failure.

Second, to observe the effect of native baroreflex function, we closed the native baroreflex loop. The laboratory computer in real time commanded the power amplifier to make carotid sinus BRP identical with SAP by means of a digital-to-analog converter while digitizing SAP at a rate of 2 kHz through the analog-to-digital converter.

Third, to evaluate the efficacy of the BBS, we activated the BBS in the model of central baroreflex failure.

### Statistical Analysis

The SAP responses to head-up tilt tests were analyzed by a mixed model of ANOVA. A post hoc analysis for multiple comparisons was performed by a Scheffé procedure. Differences were considered significant at $P<0.05$. Values are expressed as mean±SD.

## Results

Shown in Figure 2A are the averaged transfer functions for the artificial vasomotor center $H_{BRP\to STM}$ for 10 rats. The gain gradually increased ≈2-fold with input frequencies. The phase spectrum showed that the input-output relation was out of phase. These characteristics were also expressed in the time-domain analysis (Figure 2B). The initial overshoot response to unit step input was found.

A representative example of the results of head-up tests showed the performance of the BBS (Figure 3). While BRP was kept constant at the same level of supine SAP, HUT

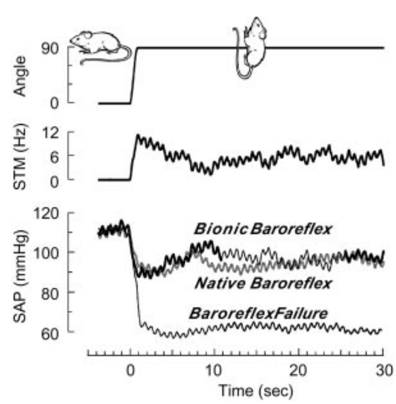


**Figure 3.** Representative example of on-line, real-time operation of bionic baroreflex system during HUT. In a model of central baroreflex failure (thin line), carotid sinus baroreceptor pressure was kept constant at the level of SAP in a supine position after HUT. When the bionic baroreflex system was inactive, SAP fell rapidly and severely immediately after HUT. On the other hand, while the bionic baroreflex system was activated (thick line), such an SAP fall was buffered as if the native baroreflex function (outlined line) was restored. While sensing changes in SAP, the bionic baroreflex system automatically computed the frequency of STM of the sympathetic nerves and drove a stimulator. Fine regular oscillation observed in SAP was ascribed to respiration. Oscillatory changes at a cycle of ≈4 seconds were found in SAP during native baroreflex and in STM and SAP during bionic baroreflex. A tilt angle was expressed by the degrees. See text for details.

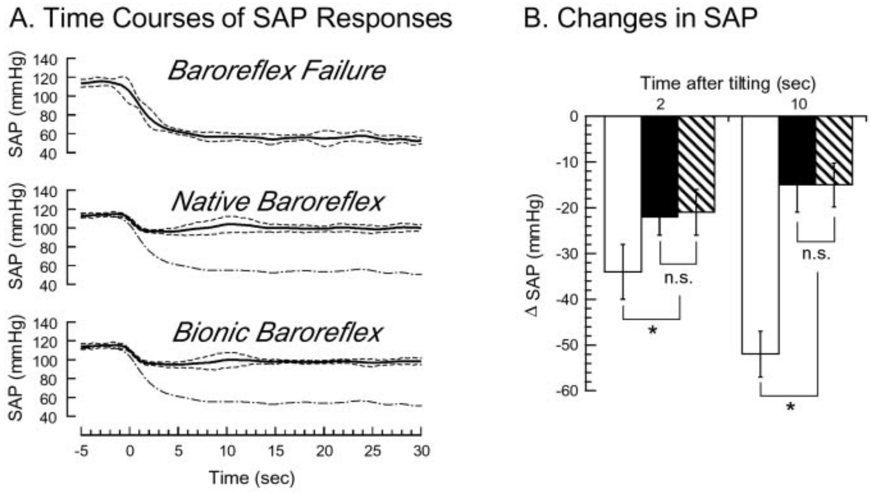


**Figure 4.** A, Plots showing time courses of SAP in a model of central baroreflex failure, native baroreflex, and bionic baroreflex. HUT was made at time 0. SAP responses by the bionic baroreflex system were similar to those by the native baroreflex system. For comparison, mean data during no baroreflex are also shown by dotted broken lines. B, Graph showing changes in SAP (ΔSAP) before and after HUT. In the model of central baroreflex failure (open column), HUT reduced SAP by 34±6 mm Hg in 2 seconds and by 52±5 mm Hg in 10 seconds. No significant difference in ΔSAP between the native (closed column) and bionic baroreflex systems (striped column) was found at 2 or 10 seconds. Data are shown as mean±SD for 10 rats. *$P<0.05$.

produced a rapid progressive fall in SAP by 40 mm Hg in only 2 seconds. By contrast, while the BBS was activated, it automatically computed STM and appropriately stimulated the sympathetic nerves to quickly and effectively attenuate the SAP drop, as if the native baroreflex function had been restored almost perfectly. In addition, the BBS automatically mimicked the low-frequency oscillation of SAP by the oscillatory change at ≈4 seconds in STM.

Figure 4 summarizes the results obtained from 10 rats, demonstrating effectiveness of the BBS performance in buffering SAP fall in response to HUT. In the model of central baroreflex failure, HUT produced a rapid progressive hypotension. However, while the BBS was activated, the time courses of the SAP responses were found to be similar to those of the native baroreflex system (Figure 4A). To make a statistical comparison of the SAP responses under the three experimental conditions, we analyzed the SAP changes before and at 2 and 10 seconds after HUT. In the model of central baroreflex failure, abrupt HUT reduced SAP by 34±6 mm Hg in 2 seconds and by 52±5 mm Hg in 10 seconds (Figure 4B). During real-time execution of the BBS, on the other hand, the fall in SAP was 21±5 mm Hg at 2 seconds and 15±6 mm Hg at 10 seconds after HUT. Such an SAP response to HUT during the real-time execution of the BBS was statistically indistinguishable from that during functioning of the native baroreflex.

## Discussion

### Baroreflex Function in Head-Up Tilting

Our experimental preparations for alternating between open-loop and closed-loop conditions of the baroreflex system even after isolation of baroreceptor regions and for servocontrolling BRP at any level allowed us to quantitatively evaluate the native baroreflex function in each animal. Although the primary purpose of the present study was to evaluate the efficacy of the BBS in restoring SAP against orthostatic hypotension in the model of central baroreflex failure, our results, as a byproduct, highlighted the quickness and effectiveness of native baroreflex function in buffering the effect of HUT on SAP.

Our previous study[6] revealed that the effectiveness of baroreflex in attenuation of the effect of external disturbance depends on the operating point of the baroreflex system before the disturbance. Therefore, it would be difficult to evaluate the open-loop gain of the baroreflex system for attenuation of the effect of HUT on SAP by open-loop approaches such as baroreceptor deafferentation and autonomic blockade. Because baroreceptor deafferentation elevates and autonomic blockade lowers the baseline level of SAP at supine, the operating point of the baroreflex system could deviate from a physiological range. On the other hand, in the present study, the predisturbance operating point was kept at the equal level between open-loop and closed-loop conditions. From Figure 4B and the following equation, the open-loop gain G was estimated to be ≈2.5.

$$G=\frac{\Delta SAP_{open}}{\Delta SAP_{closed}}-1$$

where $\Delta SAP_{open}$ and $\Delta SAP_{closed}$ are the SAP changes produced by HUT under open-loop and closed-loop conditions, respectively. The estimate of the open-loop gain for attenuation of the effect of HUT on SAP was consistent with our previous results[6,24] of the maximum gain estimated from the BRP-SAP relation under the open-loop conditions. Therefore, the present study supports our previous conclusion[6] that the arterial baroreflex functioning in a supine position is optimized in terms of gain and displays its best ability to stabilize arterial pressure against an external disturbance.

A recent study by Furlan et al[29] indicated that low-frequency (≈0.1 Hz) oscillatory patterns of sympathetic neural discharge and SAP are enhanced during HUT in humans. The low-frequency oscillations at 0.2 to 0.6 Hz in rats is known to correspond to those at 0.1 Hz in humans.[30] Interestingly, as shown in Figure 3, oscillatory changes at 0.25 Hz were found in STM and SAP during bionic baroreflex as well as in SAP during native baroreflex but not in SAP during no baroreflex. Therefore, the baroreflex feedback mechanism would be important in the genesis of such a physiological oscillation of SAP at the low frequency. To clarify a detailed mechanism for the genesis of the low-frequency oscillation of SAP, however, more systematic and quantitative studies are needed.

## Clinical Implications

Two important challenges accompany the prospect of future development of the BBS for central baroreflex failure: (1) Hardware for clinical use is required, for example, a pressure sensor, an electrical stimulator, and stimulating electrodes; (2) A standardized software paradigm prescribing precisely how the bionic vasomotor center should determine STM in response to changes in SAP needs to be established. Fortunately, certain difficulties posed by these challenges have already been addressed in other areas of clinical practice to some degree and may be readily adaptable for use with the BBS. For example, a tonometer[31] has been developed as a noninvasive continuous monitor of SAP. Implantable pulse generators such as cardiac pacemakers can serve as permanent electrical stimulators. Also, implantable wire leads for nerve stimulation[32] and epidural catheters[33] for spinal stimulation have been approved for the long-term treatment of some neurological disorders and for the chronic therapy of pain control. Finally, we could confirm the efficacy of the BBS even though the present data were obtained from experimental animals and therefore we enthusiastically affirm not only that we can but that we should develop the BBS as a new therapeutic modality for treatment of severe orthostatic intolerance in central baroreflex failure such as Shy-Drager syndrome, baroreceptor deafferentation, and traumatic spinal-cord injuries in future.

## Limitations

The vasomotor center of the arterial baroreflex is affected by other autonomic centers such as respiratory centers and higher-order centers such as the limbic-hypothalamic systems and also receives various afferents such as cardiopulmonary receptors.[34] Anesthetic agents used in the present study and artificial ventilation could also affect the dynamic properties of arterial baroreflex. In the present study, we ignored these effects. Thus, further investigation is needed for clarifying the native baroreflex function and developing the truly "bionic" baroreflex system.

## Acknowledgments

This study was supported by research grants from Uehara Memorial Foundation, Suzuken Memorial Foundation, and Tateisi Science and Technology Foundation.

## References

1. Schmidt RM, Kumada M, Sagawa K. Cardiac output and total peripheral resistance in carotid sinus reflex. *Am J Physiol*. 1971;221:480–487.
2. Guyton AC, Coleman TG, Granger HJ. Circulation. overall regulation. *Ann Rev Physiol*. 1972;34:13–46.
3. Robertson D. Diagnosis and management of baroreflex failure. *Primary Cardiol*. 1995;21:37–40.
4. Malliani A, Pagani M, Lombardi F, et al. Cardiovascular neural regulation explored in the frequency domain. *Circulation*. 1991;84:482–492.
5. Shamsuzzaman AS, Somers VK. Cardiorespiratory interactions in neural circulatory control in humans. *Ann N Y Acad Sci*. 2001;940:488–499.
6. Sato T, Kawada T, Inagaki M, et al. A new analytical framework for understanding the sympathetic baroreflex control of arterial pressure. *Am J Physiol*. 1999;276:H2251–H2261.
7. Shy M, Drager GA. A neurological syndrome associated with orthostatic hypotension: a clinico-pathologic study. *Arch Neurol*. 1960;3:511–527.
8. Consensus Committee of the American Autonomic Society and the American Academy of Neurology. Consensus statement on the definition of orthostatic hypotension, pure autonomic failure, and multiple system atrophy. *Neurology*. 1996;46:1470.
9. Schatz IJ. Farewell to the "Shy-Drager syndrome." *Ann Intern Med*. 1996; 125: 74–75.
10. Goldstein DS, Holmes C, Cannon RO III, et al. Sympathetic cardioneuropathy in dysautonomias. *N Engl J Med*. 1997;336:696–702.
11. Onrot J, Wiley RG, Fogo A, et al. Neck tumour with syncope due to paroxysmal sympathetic withdrawal. *J Neurol Neurosurg Psychiatry*. 1987;50:1063–1066.
12. Lee HT, Brown J, Fee WE Jr. Baroreflex dysfunction after nasopharyngectomy and bilateral carotid isolation. *Arch Otolaryngol Head Neck Surg*. 1997;123:434–437.
13. Frankel HL, Mathias CJ. Severe hypertension in patients with high spinal cord lesions undergoing electro-ejaculation: management with prostaglandin $E_2$. *Paraplegia*. 1980;18:293–299.
14. Matthews JM, Wheeler GD, Burnham RS, et al. The effects of surface anaesthesia on the autonomic dysreflexia response during functional electrical stimulation. *Spinal Cord*. 1997;35:647–651.
15. Wilcox CS, Puritz R, Lightman SL, et al. Plasma volume regulation in patients with progressive autonomic failure during changes in salt intake or posture. *J Lab Clin Med*. 1984;104:331–339.
16. Mehlsen J, Boesen F. Substantial effect of acute hydration on blood pressure in patients with autonomic failure. *Clin Physiol*. 1987;7:243–246.
17. Kristinsson A. Programmed atrial pacing for orthostatic hypotension. *Acta Med Scand*. 1983;214:79–83.
18. Bannister R, da Costa DF, Hendry WG, et al. Atrial demand pacing to protect against vagal overactivity in sympathetic autonomic neuropathy. *Brain*. 1986;109:345–356.
19. Kachi T, Iwase S, Mano T, et al. Effect of L-threo-3,4-dihydroxyphenylserine on muscle sympathetic nerve activities in Shy-Drager syndrome. *Neurology*. 1988;38:1091–1094.
20. Obara A, Yamashita H, Onodera S, et al. Effect of xamoterol in Shy-Drager syndrome. *Circulation*. 1992;85:606–611.
21. Sato T, Kawada T, Shishido T, et al. Novel therapeutic strategy against central baroreflex failure: a bionic baroreflex system. *Circulation*. 1999; 100:299–304.
22. Marmarelis PZ, Marmarelis VZ. *Analysis of Physiological Systems: The White-Noise Approach*. New York, NY: Plenum; 1978.
23. Sato T, Kawada T, Shishido T, et al. Dynamic transduction properties of in situ baroreceptors of rabbit aortic depressor nerve. *Am J Physiol*. 1998;274:H358–H365.
24. Sato T, Kawada T, Miyano H, et al. New simple methods for isolating baroreceptor regions of carotid-sinus and aortic-depressor nerves in rats. *Am J Physiol*. 1999;276:H326–H332.
25. Gabella G. Autonomic nervous system. In: Paxinos G, ed. *The Rat Nervous System*. 2nd ed. San Diego, Calif: Academic Press; 1995:81–103.
26. Hainsworth R, Karim F. Responses of abdominal vascular capacitance in the anaesthetized dog to changes in carotid sinus pressure. *J Physiol (Lond)*. 1976;262:659–677.
27. Carneiro JJ, Donald DE. Blood reservoir function of dog spleen, liver, and intestine. *Am J Physiol*. 1977;232:H67–H72.
28. Ikeda Y, Kawada T, Sugimachi M, et al. Neural arc of baroreflex optimizes dynamic pressure regulation in achieving both stability and quickness. *Am J Physiol*. 1996;271:H882–H890.
29. Furlan R, Porta A, Costa F, et al. Oscillatory patterns in sympathetic neural discharge and cardiovascular variables during orthostatic stimulus. *Circulation*. 2000;101:886–892.
30. Japundzic N, Grichois ML, Zitoun P, et al. Spectral analysis of blood pressure and heart rate in conscious rats: effects of autonomic blockers. *J Auton Nerv Syst*. 1990;30:91–100.
31. Sato T, Nishinaga M, Kawamoto A, et al. Accuracy of a continuous blood pressure monitor based on arterial tonometry. *Hypertension*. 1993;21:866–874.
32. Reid SA. Surgical technique for implantation of the neurocybernetic prosthesis. *Epilepsia*. 1990;31(suppl 2):S38–S39.
33. Shimoji K, Hokari T, Kano T, et al. Management of intractable pain with percutaneous epidural spinal cord stimulation: differences in pain-relieving effects among diseases and sites of pain. *Anesth Analg*. 1993; 77:110–116.
34. Furlan R, Jacob G, Palazzolo L, et al. Sequential modulation of cardiac autonomic control induced by cardiopulmonary and arterial baroreflex mechanisms. *Circulation*. 2001;104:2932–2937.